# TIME TRANSFER FROM COMBINED ANALYSIS OF GPS AND TWSTFT DATA

**Pascale Defraigne**
**Royal Observatory of Belgium (ROB)**
**Avenue Circulaire, 3, B-1180 Brussels, Belgium**
**E-mail: *p.defraigne@oma.be***

**M. Carmen Martínez[1] and Z. Jiang[2]**
**[1]University of Alicante, Spain, E-mail: *carmen.martinez@ua.es***
**[2]Bureau International des Poids et Mesures, France, E-mail: *zjiang@bipm.org***

**Abstract**

***This paper presents the time transfer results obtained from the combination of GPS data and TWSTFT data. Two different methods are used for the combination: a first one (named CV+TW) is based on a least-squares analysis of GPS code and carrier-phase measurements in common view, constrained by TWSTFT data. Using the Vondrak-Cepek algorithm, the second approach (named PPP+TW) combines the TWSTFT time transfer data with the GPS clock solutions computed with Precise Point Positioning. Combining GPS and TWSTFT considerably increases the robustness of the accurate time transfer result due to the complete independence between the two spatial techniques. Both combination methods provide a time transfer solution which benefits from the high short-term stability and high resolution of the GPS data and the high accuracy of the TWSTFT data. The PPP+TW solution is continuous, while some discontinuities exist in the solution CV+TW, due to the noise and diurnal perturbation in the TW data. In general, the solutions obtained with both methods agree well with each other. The r.m.s. of the differences between the results remains below 300 picoseconds for the links investigated.***

## INTRODUCTION

The two main techniques presently used for accurate time transfer are « Geodetic time transfer » based on the joint analysis of GPS code and carrier-phase measurements, together with a consistent modeling of these measurements and «Two-Way Satellite Time and Frequency Transfer » (TWSTFT), which is based on measurements of transit time of signals traveling symmetric ways between the two clocks to be compared. While geodetic time transfer is widely recognized for its high frequency stability (see, for instance, **[1-3]**), and its high resolution, it is, however, limited by the colored signature of the code noise, affecting the medium-term stability of the solution and inducing possible discontinuities at the day boundaries **[4]**. Furthermore, the calibration of the GPS equipment is presently limited to 5 ns, as set in the $u_B$ uncertainty in the BIPM Circular T. The carrier phases themselves allow one to give a precise signal evolution, but as these measurements contain an unknown initial ambiguity (integer number of cycles), the code measurements are necessary to determine the absolute offset between the clocks.

In parallel, TWSTFT (TW hereafter) is a time transfer method completely independent of GPS, which has been evaluated since 1999 by the BIPM (Bureau International des Poids et Mesures) as an alternative technique to generate the International Atomic Time (TAI). TW is calibrated and the measurements may be performed with sub-nanosecond uncertainty and reproducibility **[5]** as set forth in the $u_B$ uncertainty in the BIPM Circular T. The long-term performance of TW has already been shown to be equivalent to that of geodetic time transfer (see, for instance, **[6]**). However, TW measurements may be disturbed by a diurnal oscillation of 1 to 3 ns peak to peak **[7]** and its resolution its poor, with one point every 2 hours in general.

The TAI time transfer network is highly redundant: all the TW time links are back up with GPS. A post-combination of the time transfer solutions obtained with these two kinds of links was proposed in **[7,8]**, based on the Vondrak-Cepek combined smoothing algorithm **[11]**. An alternative method was presented in **[12]**, which directly combines the TWSTFT data and GPS data (code and carrier-phase measurements in common view) of such redundant links in a common least-squares analysis. The two kinds of combined solutions keep the advantages of both systems, i.e. an accuracy corresponding to the accuracy of the TW and a high resolution and a high frequency stability assigned by the GPS carrier-phase measurements.

The first section of this paper will focus on the algorithms and methodologies used for the combinations, and the second section will discuss the differences between the results obtained in both approaches.

## COMBINATION STRATEGIES

### POST-COMBINATION (PPP+TW)

The method of post-combination is based on Vondrak-Cepek combined smoothing **[11]**, improving the Whittaker-Robinson-Vondrak smoothing that suppresses the high frequency noises present in a series of unequal uncertainty and unequally spaced observations. The main principle is to smooth a function with given derivatives. In our case, the given TW data are combined with the derivative of the GPS time transfer solutions computed in a PPP approach. The curve of the combined result is smooth and continuous even while one of the raw data sets are affected by the jumps and discontinuities. However, the combination may be deformed locally when these faults happen. See the following discussion. The procedure is detailed in **[8]**.

### COMMON-VIEW CONSTRAINT BY TW DATA (CV+TW)

The approach consists in inserting the TW data as additional observation equations in a least-squares analysis of GPS code and carrier-phase data. As the TW data directly provide the time link between two stations, they can only be combined with single differences of GPS observations, i.e. differences between the simultaneous observations of a same satellite in both stations. The Atomium software **[9]**, initially developed for GPS Precise Point Positioning (PPP or zero differences), was therefore adapted to use single differences of GPS code and carrier-phase observations.

Atomium is based on a weighted least-squares approach; the observations are ionospheric-free combinations of dual-frequency GPS code (named $P_3$) and carrier-phase (named $\phi_3$) observations, and the software, in PPP mode, determines the station position for the whole day, the receiver clock at each epoch, and tropospheric delays at a given rate (2 hours in our case). The procedure has been described in **[12]**, and will be here only summarized.

The single differences in GPS are performed by subtracting the observation equations of two different stations with the same satellite in view at the same time. This technique allows canceling the satellite clock bias, assuming that the nominal times of observation of the satellite by the two stations are the same. Denoting the stations by *p* and *q* and the satellite by *i*, the single-difference code and carrier-phase equations are:

$$\begin{aligned}(P_3)^i_p - (P_3)^i_q &= \rho^i_{pq} + c\Delta t_{pq} + (\tau_p - \tau_q) + \varepsilon_P \\ (\phi_3)^i_p - (\phi_3)^i_q &= \rho^i_{pq} + c\Delta t_{pq} + (\tau_p - \tau_q) + N^i_{pq}\lambda + \varepsilon_\phi\end{aligned} \qquad (1)$$

where $\rho^i_{pq}$ is the difference between the geometric ranges between stations *p* and *q* and the satellite, $\Delta t_{pq}$ is the synchronization error between the receiver clocks in stations *p* and *q*, *c* is the vacuum speed of light, $N^i_{pq}$ is the total phase ambiguity of the phase difference $(\phi_3)^i_p - (\phi_3)^i_q$, $\tau$ is the tropospheric delay, and $\varepsilon_P$ and $\varepsilon_\phi$ are the noise terms for the code and carrier-phase combinations.

These observation equations are completed by adding the TW measurements. As the hardware delay of the TW equipment (total delay between the clock and the measurement point) is different from the hardware delay of the GPS equipment, it is necessary to estimate an additional parameter which is the offset between the TW and GPS data, and which is considered constant for each day processed. Note that this parameter also contains the long-term variations of the GPS code data, which are due to some site effect **[4]**, so that it can vary with time. The TW hardware delay is considered as constant with time and the parameter *k* is, therefore, considered to be the sum of the offset between the TW hardware delay and the GPS hardware delay plus the average GPS code error during the day analyzed. The additional observation equations can, therefore, be written as:

$$c\Delta t^{TW}_{t_k pq} = c\Delta t^{GPS}_{t_k pq} + k \qquad (2)$$

for each observation epoch $t_k$ where a TW measurement exists.

The weights for the GPS code and carrier-phase data are set to 1 and $10^4$, as the noise level of the phase measurements is about 100 times smaller than the corresponding noise level of the code observable. These weights are then multiplied by the $\sin^2$ of the elevation for each satellite measurement. The level of noise of the TW measurements (in Ku-band) is approximately 3 times smaller than the GPS code measurements noise, so that the weight of the TW equations is fixed to be 9 times the average noise given to the code data. Thanks to this weight repartition, the high stability given by GPS carrier phases is maintained, but the mean absolute clock synchronization error over 1 day is determined by the TW data rather than by the P-code data. The long-term instability due to the P-code noise in the GPS-only time and frequency transfer will, therefore, be mitigated.

## *IMPROVEMENTS IN THE METHOD OF COMMON-VIEW CONSTRAINT BY TW DATA*

For long baselines, the number of GPS satellites in common visibility at each epoch from both stations is reduced. Moreover, the quality of the GPS phase and code measurements may be lower, because the satellites in common visibility for both stations are those which are at the low elevations, so that the signal is more affected by the atmosphere and multipath. The quality of the combined solution is, therefore, reduced because of the reduced quality of the GPS single differences. This was illustrated in our previous paper **[12]**. In order to overcome that problem, intermediary GPS stations have been introduced in the analysis. These stations do not participate in any TW measurements, but allow the reduction of the GPS baselines and to improvement of the clock solution based on GPS single differences.

In that case, the position of one station is fixed, and all other positions are determined together with the clock solutions. For a set of four stations *(p,r,s,q)*, i.e. using two intermediary stations *r* and *s* for the link *pq*, corresponding to the TW link, the new observations equations are firstly equation (1) applied to receiver pairs *p*-*r*, *r*-*s* and *s*-*q*, and secondly equations (2), which now read:

$$c\Delta t^{TW}_{t_k pq} = c\Delta t^{GPS}_{t_k pr} + c\Delta t^{GPS}_{t_k rs} + c\Delta t^{GPS}_{t_k sq} + k \qquad (3)$$

for each observation epoch $t_k$ where a TW measurement exists.

The introduction of two intermediary stations provides more data per epoch in each of the three single differences of the analysis, and the satellites in common visibility are at higher elevation, so that the data are less affected by multipath, the tropospheric delay is better determined for each station, and the solution is not deformed. Figure 1 illustrates this conclusion with the link USNO-PTB. The solution with either only the stations of the link (SD(2)), or also with the two intermediary stations STJO and OPMT (SD(4)), is depicted togheter with the reference classical geodetic time transfer solution, (USNO-IGST)-(PTB-IGST), for a 3-day sample time period in April 2008. A clear deformation of the solution within each daily batch is observed in SD(2). Indeed, the standard deviation of the differences with the IGS time transfer solution is 285 picoseconds (ps), with a maximum of 1 ns reached in the middle of MJD 54566, while the differences of IGS and SD(4) have a standard deviation of 170 ps, i.e. a reduction of 40% with respect to SD(2), and the maximum difference is 0.52 ns.

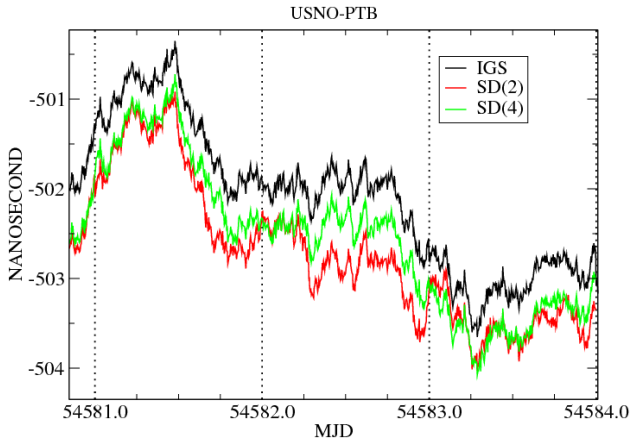


Figure 1. Comparison between the solutions obtained for USNO-PTB using the single difference analysis with or without two intermediary stations.

## RESULTS OF COMBINATIONS

Two separate links have been investigated for the comparison between the least-squares analysis constrained by TW data (CV+TW) and the combined smoothing (PPP+TW) approaches: NIST-PTB and USNO-PTB. As these links correspond to long baselines, the CV+TW solutions have been computed using two intermediary stations. The networks are, respectively, using the IGS names of the stations (see Figure 2), NIST-STJO-OPMT-PTBB, and USN3-STJO-OPMT-PTBB.

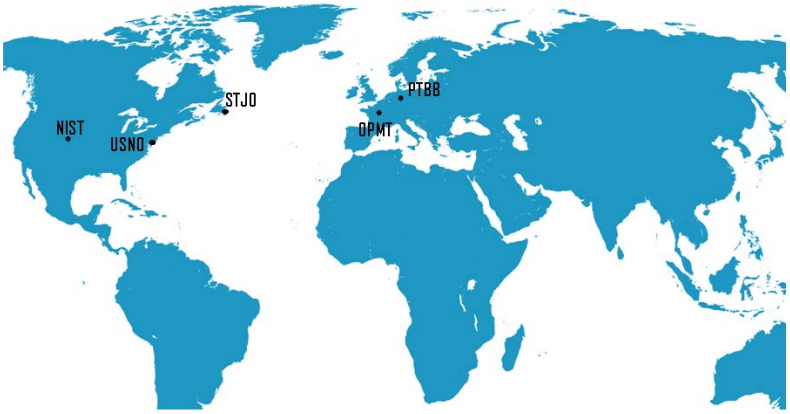


Figure 2. Distribution of the stations used for the CV+TW approach for the two transatlantic time transfer baselines NIST-PTB and USNO-PTB.

The analysis has been performed on a period of 1 month, April 2008, during which TW data are available. The link NIST-PTB is presented in Figures 3 and 4.

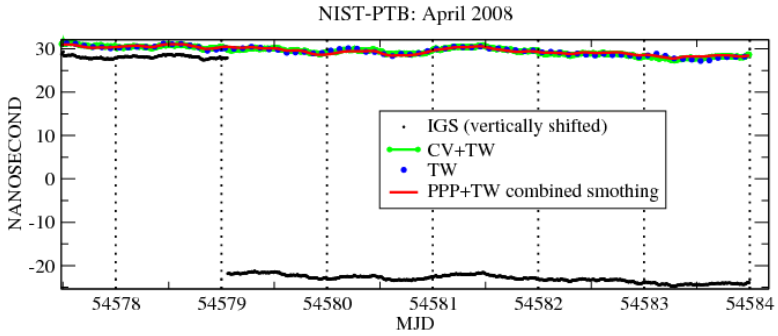


Figure 3. Continuity of the combined solution PPP+TW and CV+TW in case of GPS hardware delay changes as observed for NIST-PTB.

The large jump observed in Figure 3 at about MJD 54579 is due to a jump of about 50 nanosecond in the GPS clock solution of NIST; it is not due to any clock variation, as the TW data are continuous at that epoch, but it is rather due to a sudden change in the hardware delay of the GPS equipment at NIST. The two combined solutions, still showing the clock signal given by the GPS carrier phases, are continuous at that epoch, thanks to the calibration with TW data, which are continuous. Furthermore, analyzing the 3 weeks before the jumps (Figure 4), one can see that the two important jumps appearing in the IGS solution (or in any classical GPS geodetic time transfer solution) at MJD 54559 and 54573 do not produce apparent discontinuities in the combined solutions. The reasons for the jumps in the GPS-only solutions are not very clear, probably due to some variations of the pseudorange measurements in NIST at these epochs. In the right plot of Figure 4, the PPP+TW combination (red line) does not follow exactly the plot of TW. In fact, the PPP used in the combination is affected by jumps, discontinuities, and drifts. This comes from the PPP analysis, which was performed using the NRCan software **[13]** on a 1-month data batch, which induces this kind of variations in case of pseudorange jumps, as already shown in **[9]**. Figure 4a illustrates the erroneous PPP corresponding to the related period. The PPP+TW combination considerably reduces these defaults in PPP, but a remaining drift remains in the solution.

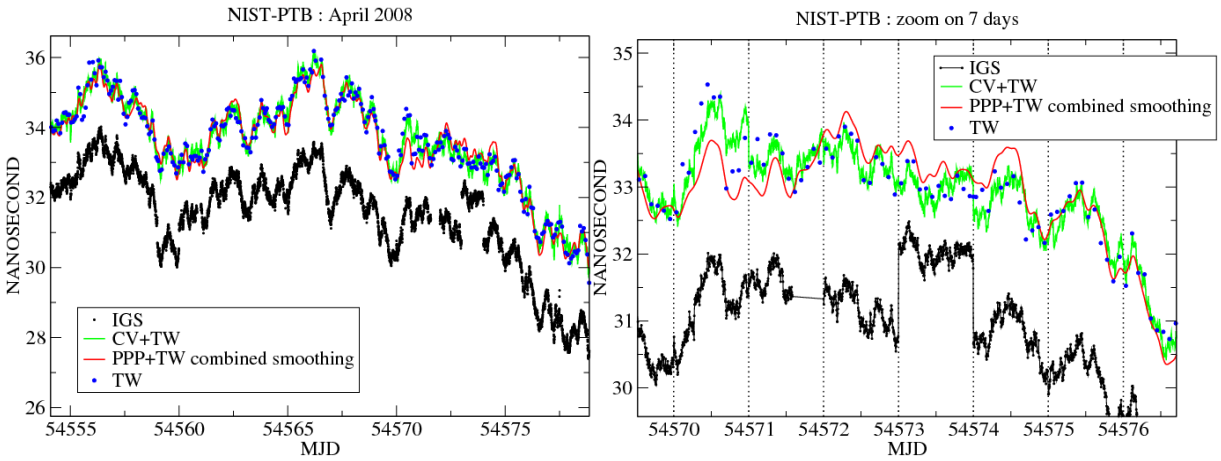


Figure 4. Comparison between the PPP+TW combined smoothing and the GPS CV constrained by the TW data for the link NIST-PTB in April 2008 (left) and over 1 week (right).

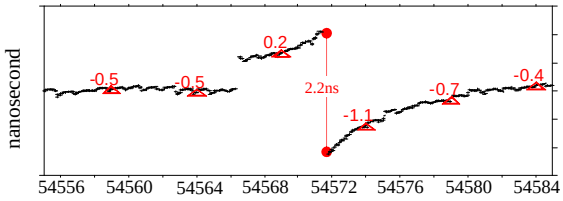


Figure 4a. Erroneous PPP solution at PTB used for the PPP+TW combination corresponding to the red curve in the right plot in Figure 4. Discontinuities, drifts, and jumps up to 2.2 ns happened between MJD 54564-54572.

Comparing the solutions obtained with CV+TW and PPP+TW, it can be observed that the noise level of the CV+TW is larger than the one of PPP+TW. The noise of the CV+TW solution is indeed the noise level of the GPS clock solutions, i.e. about 10 ps, while the PPP+TW approach contains a smoothing reducing the short-term noise. However, the two solutions coincide with an average difference of 23 ps, and a standard deviation of the differences of 258 ps. The maximum difference is shown in the right hand part of Figure 3, where it reaches 1 ns at the end of MJD 54570. The cause was explained in the above paragraph.

An important difference between the two solutions is the continuity of the solution across the day boundaries. In the CV+TW solution, the GPS and TW data are analyzed in 1-day data batches. For each day, the solution is calibrated by the TW data (about 12 data per day), while the shape of the curve is given by the GPS phase measurements. The 1-day average of the differences between the CV+TW solution and the TW data is, therefore, very close to zero, which is not always the case for the PPP+TW solution. Furthermore, due to the calibration of the CV+TW solution on the TW data of the day, some jumps can appear at the day boundaries due to the noise of the TW data. Sometimes, the jump of the CV+TW solution is even larger than the jump in the GPS-only solution, as seen on the right-hand part of the Figure 3 at MJD 54571.0. However, the jump in the combined CV+TW solution is always below 600 ps in this case.

The second link investigated was USNO-PTB (Figures 5 and 6), using first the Ku-band data. The two combined solutions obtained for this link coincide with an average difference of 10 ps, and a standard deviation of the differences of 174 ps. The maximum difference is shown in the right-hand part of Figure 5, where it reaches 0.721 ns at the end of MJD 54571. Similar conclusions can be drawn as for NIST-PTB concerning the calibration and the continuity of the solutions across the day boundaries. The cause for the PPP+TW combination has been explained above as due to the erroneous PPP illustrated in Figure 4a. And again, the faults in the PPP have been significantly reduced, thanks to TW data. Further investigations prove that not only the faults in GPS but also the faults in TW, such as the diurnals, are detected, corrected, or reduced **[8]**. The combination of the TW and GPS increases the robustness of the time transfer.

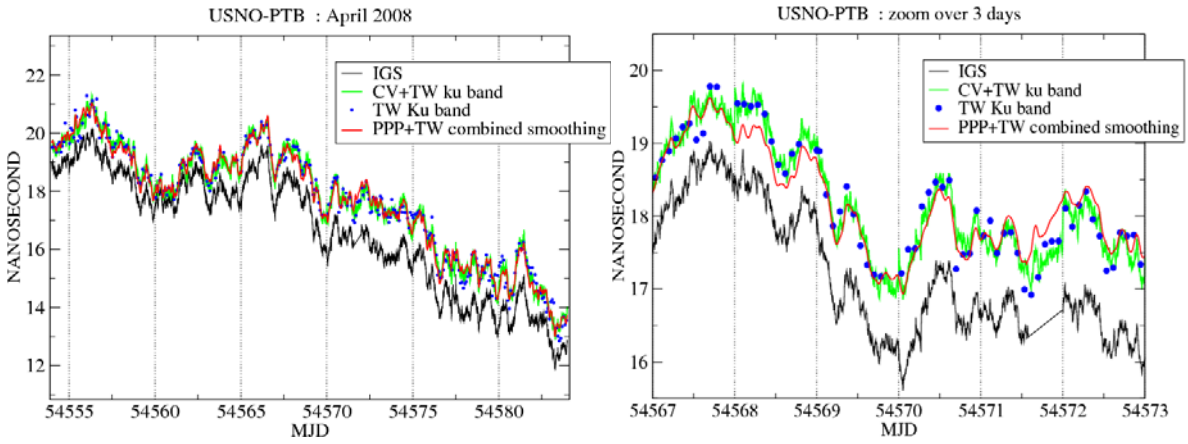


Figure 5. Comparison between the PPP+TW combined smoothing and the GPS CV constrained by the TW data for the link USNO-PTB in April 2008 (left) and over six days (right).

The link USNO-PTB exists in TW Ku band as well as TW X-band. The advantage of the X-band is the number of observations, which is 2 times larger than the number of TW data in Ku-band. The comparison between the combination obtained with the TW data in X- and Ku-bands is presented in Figure 6. During the month we have analyzed, there is a long-term variation in the differences between the TW data in X- and Ku-bands, leading to differences up to 2 nanoseconds; this trend exists, of course, also between the combined solutions obtained with TW data in X- and Ku-bands.

The combination CV+TW using X band data produces, in general, a solution with day-boundary jumps smaller than CV+TW using Ku-band data (Figure 7), as there are twice more TW points to calibrate the solution, and they are not affected by the diurnal signal. However, the average of the jump sizes is not significantly lower (231 ps and 198 ps for Ku- and X-bands, respectively).

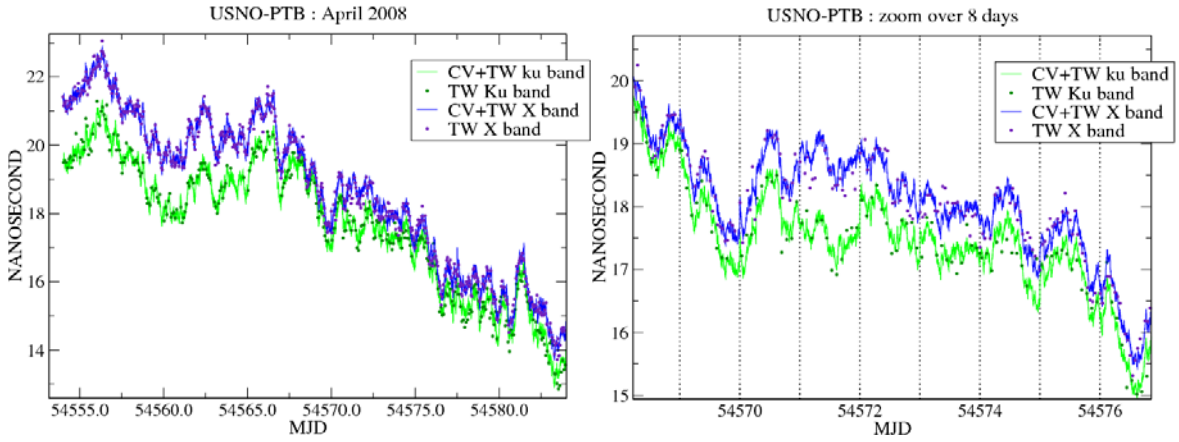


Figure 6. Comparison between the combined solutions obtained with the CV+TW approach using either TW data in Ku-bands or TW data in X-band.

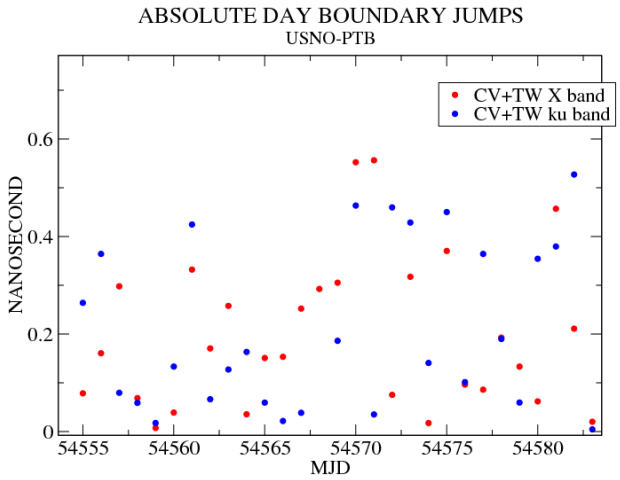


Figure 7. Comparison between the day-boundary jump amplitudes of the combined CV+TW solutions using either TW data in Ku-bands or TW data in X-band.

To sum up, Table 1 shows some statistics of the differences between the results obtained with each combination method and the TW data for the two links investigated. The corresponding differences are plotted in Figure 8. The average of the differences between the CV+TW method and TW remains close to zero, as it was expected, and it is also lower than the average of the differences between PPP-TW and TW, due to the different way the TW data are used for the combination. For the same reason, the standard deviations of these differences are larger for PPP+TW than for CV+TW (see Table 1). The differences between PPP+TW and CV+TW are plotted in Figure 9. Their average and standard deviations were given previously in the text. We can observe that the differences for the two links investigated have very similar amplitudes and shapes.

Table 1. Statistic summary of the differences between TWSTFT and, either the combined smoothing or the GPS CV constrained by the TW data, for the links NIST-PTB, and USNO-PTB in April 2008.

| | **(PPP+TW) – TWSTFT** | | **(CV+TW) - TWSTFT** | |
|---|---|---|---|---|
| | average | std. deviation | average | std. deviation |
| **NIST-PTB** | 19 ps | 298 ps | <0.001 ps | 201 ps |
| **USNO-PTB** | 11 ps | 276 ps | < 0.001 ps | 236 ps |

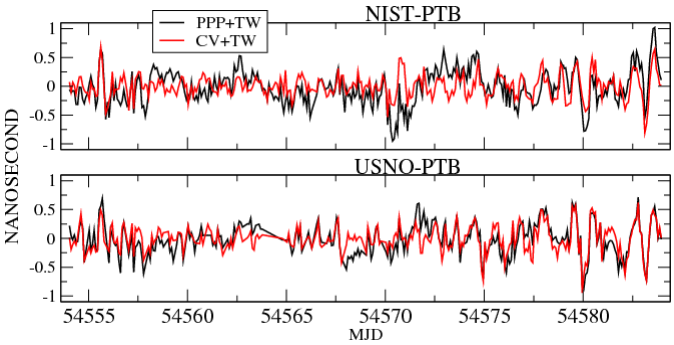


Figure 8. Differences between TWSTFT and either the PPP-TW combined smoothing or the GPS CV+TW constrained by the TW data for the links NIST-PTB and USNO-PTB in April 2008.

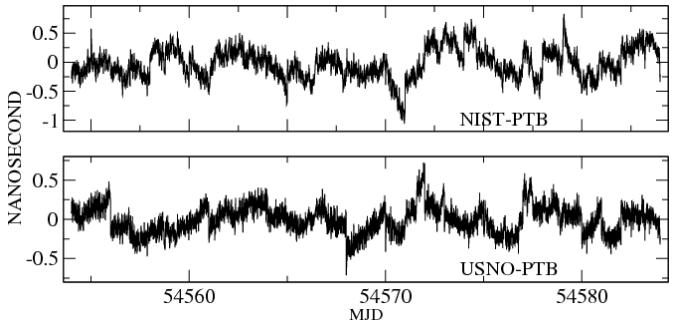


Figure 9. Differences between the PPP-TW combined smoothing and the GPS CV+TW constrained by the TW data solutions for the links NIST-PTB and USNO-PTB in April 2008.

## RESULTS FOR A TIME LINK WITH HIGH NOISE IN TWSTFT DATA

As pointed in the previous paragraphs, the CV+TW method is significantly affected by the TW short-term behavior, producing undesiderable day-boundary jumps in the solution. In order to illustrate that, the short-baseline link IT-PTB, for which the TW data are noisy in April 2008, has been investigated. As this concerns an intra-continental baseline, no intermediary station was included in the analysis. The combined CV+TW solution is presented in Figure 10. One can observe that the noise in the TW data induces a large dispersion of the TW data points around the combined solution. The standard deviation of

the differences between the CV+TW solution and the TW data is at the level of 500 ps, which is significantly higher than the standard deviation of about 250 ps obtained for the two previous links. A further consequence of the noisy TW data used for the CV+TW combination is the possible presence of important discontinuities at the day batch boundaries. This is illustrated in the right part of Figure 10, where the jump in MJD 54568.0 reaches an amplitude of 1 nanosecond, while the GPS-only was perfectly continuous at that epoch. The continuity of the CV+TW combined solution depends, therefore, highly on the noise of the TW data used for the analysis.

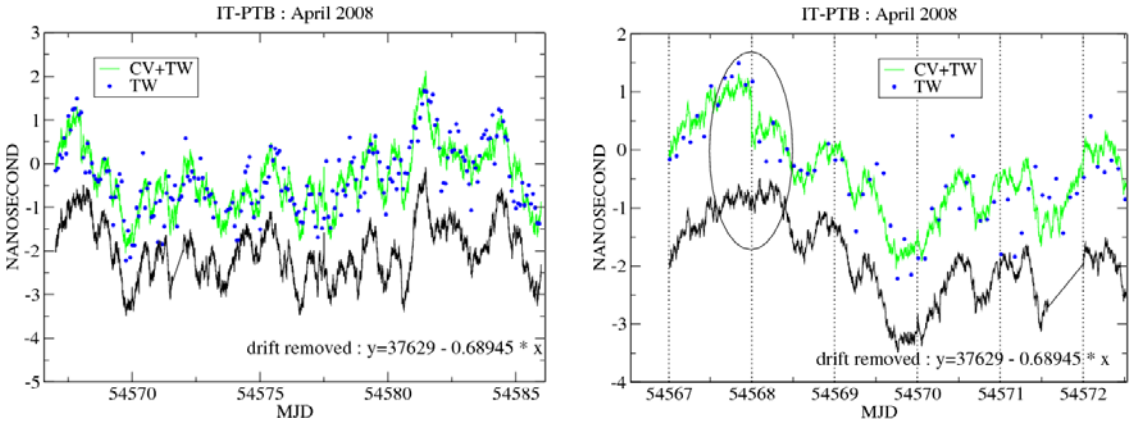


Figure 10. Comparison between the IGS solution and the GPS CV constrained by the TW data in the case of noisy TW data.

## CONCLUSIONS

This study presented the comparison between two different approaches of a TWSTFT and GPS combined time transfer solution. Based on entirely different principles, they both provide a combined time transfer solution which benefits from the high short-term stability and high resolution of the GPS data, and the high accuracy of the TW data. At present, the accuracy of the TW data is indeed 5 times higher than the accuracy of the GPS code data. The first method is a direct combination of GPS with TWSTFT. It performs a least-squares analysis of single differences (common view) of GPS code and carrier-phase measurements constrained by TW data. The second method is based on a postprocessing of TW data with the rate of a PPP time transfer solution, using a smoothed Vondrak-Cepek algorithm. Both methods have been validated on different time links, and were shown successful for all of them. The methods developed here are successful in reducing the large day-boundary discontinuities, either due to GPS hardware delay changes, or due to the colored signature of the noise of GPS codes, that exist in some clock solutions obtained with geodetic time transfer. For the two links investigated (NIST-PTB and USNO-PTB), the differences between the two combined methods are always smaller than 1 nanosecond; the mean difference is at the level of some ps with an r.m.s. smaller than 300 ps. These differences are of the same order of magnitude as the differences between the TW data in X-band or in Ku-band. The postprocessing method provides a continuous solution, while some discontinuities at the day batch boundaries exist in the solution obtained from GPS least squares constrained by TW data. However, thanks to the constraint, the average of the differences between the constrained solution and the TW data is very close to zero, which is not always the case for the postprocessed combined solution for which, to guarantee the continuity, there would be deformation up to half a nanosecond with respect to the TW data.

TW and GPS are two completely independent spatial techniques. Combination of the both increases the robustness of the accurate time transfer, which would be not reachable using only one technique. This is also a good solution for the high redundancy in the worldwide TAI time transfer network and creates the possibility of a multi-technique time and frequency transfer.

## ACKNOWLEDGMENTS

This work has been partially supported by the grants CTBPRB/2005/429 and BEFPI/2007/040 of the Consellería de Empresa, Universidad y Ciencia of the Generalitat Valenciana. The authors also acknowledge the time laboratories for the availability of the time link data and the IGS for their data and products used in this study. Quentin Baire is also acknowledged for his help with respect to the Atomium software.

## REFERENCES

**[1]** T. Schildknecht, G. Beutler, and M. Rotacher, 1990, *"Towards sub-nanosecond GPS time transfer using geodetic processing technique,"* in Proceedings of the 4th European Frequency and Time Forum (EFTF), 13-15 March 1990, Neuchâtel (Neuchâtel University), Switzerland, pp. 335-346.

**[2]** K. M. Larson, J. Levine, L. M. Nelson, and T. Parker, 2000, *"Assessment of GPS carrier-phase stability for time-transfer applications,"* **IEEE Transactions on Ultrasonics, Ferroelectrics, and Frequency Control, 47,** 484-494.

**[3]** C. Bruyninx and P. Defraigne, 2000, *"Frequency Transfer Using GPS Codes and Phases : Short and Long Term Stability,"* in Proceedings of the 31st Annual Precise Time and Time Interval (PTTI) Systems and Applications Meeting, 7-9 December 1999, Dana Point, California, USA (U.S. Naval Observatory, Washington, D.C.), pp 471-478.

**[4]** P. Defraigne and C. Bruyninx, 2007, *"On the link between GPS pseudorange noise and day-boundary discontinuities in geodetic time transfer solutions,"* **GPS solutions, 11** (4), 239-249.

**[5]** D. Piester, A. Bauch, L. Breakiron, D. Matsakis, B. Blanzano, and O. Koudelka, 2008, *"Time transfer with nanosecond accuracy for the realization of International Atomic Time,"* **Metrologia, 45,** 185-198.

**[6]** G. Petit and Z. Jiang, 2005, "Stability of geodetic GPS time transfer and their comparison to two way time transfer," in Proceedings of the 36th Annual Precise Time and Time Interval (PTTI) Systems and Applications Meeting, 7-9 December 2004, Washington, D.C., USA (U.S. Naval Observatory, Washington, D.C.), pp. 31-39.

**[7]** Z. Jiang, R. Dach, G. Petit, T. Schildnecht, and U. Hugentobler, 2006, *"Comparison and combination of TAI time links with continuous GSS carrier phase results,"* in Proceedings of the 20th European Frequency and Time Forum (EFTF), 27-30 March 2006, Braunschweig, Germany, pp. 440-447.

**[8]** Z. Jiang, G. Petit, and P. Defraigne, 2007, *"Combination of GPS carrier phase data with a calibrated time transfer link,"* in Proceedings of TimeNav'07, IEEE Frequency Control Symposium (FCS) Joint with the 21st European Frequency and Time Forum (EFTF), 29 May-1 June 2007, Geneva, Switzerland (IEEE Publication 07CH37839), pp. 1182-1187.

**[9]** P. Defraigne, N. Guyennon, and C. Bruyninx, 2007, *"PPP and Phase-Only GPS Frequency Transfer,"* in Proceedings of TimeNav'07, IEEE Frequency Control Symposium (FCS) Joint with the 21st European Frequency and Time Forum (EFTF), 29 May-1 June 2007, Geneva, Switzerland (IEEE Publication 07CH37839), pp. 904-909.

**[10]** J. Ray and K. Senior, 2005, *"Geodetic techniques for time and frequency comparisons using GPS phase and code measurements,"* **Metrologia, 42,** 215-232.

**[11]** J. Vondrak and A. Cepek, 2000, *"Combined smoothing method and its use in combining Earth orientation parameters measured by space techniques,"* **Astronomy and Astrophysics, 147,** 347-359.

**[12]** P. Defraigne and M. C. Martínez, 2008, *"Combination of TWSTFT and GPS data for time transfer,"* in Proceedings of the 22nd European Frequency and Time Forum (EFTF), 23-25 April 2008, Toulouse, France.

**[13]** J. Kouba and P. Heroux, 2001, *"Precise Point Positioning using IGS orbits and clock products,"* **GPS Solutions, 5** (2), 12–28.